

Original Article  
Comparative and  
Translational Medicine



# Induced neural stem cells from human patient-derived fibroblasts attenuate neurodegeneration in Niemann-Pick type C mice

Saetbyul Hong <sup>1</sup>, Seung-Eun Lee <sup>1</sup>, Insung Kang <sup>1</sup>, Jehoon Yang <sup>2</sup>, Hunnyun Kim <sup>2</sup>, Jeyun Kim <sup>2</sup>, Kyung-Sun Kang <sup>1,\*</sup>

<sup>1</sup>Adult Stem Cell Research Center and Research Institute for Veterinary Science, College of Veterinary Medicine, Seoul National University, Seoul 08826, Korea

<sup>2</sup>Animal Research and Molecular Imaging Center, Samsung Medical Center, Seoul 06351, Korea

 OPEN ACCESS

Received: Jun 23, 2020

Revised: Sep 25, 2020

Accepted: Oct 28, 2020

\*Corresponding author:

Kyung-Sun Kang

Adult Stem Cell Research Center and Research Institute for Veterinary Science, College of Veterinary Medicine, Seoul National University, 1 Gwanak-ro, Gwanak-gu, Seoul 08826, Korea. E-mail: kangpub@snu.ac.kr


© 2021 The Korean Society of Veterinary Science

This is an Open Access article distributed under the terms of the Creative Commons Attribution Non-Commercial License (<https://creativecommons.org/licenses/by-nc/4.0>) which permits unrestricted non-commercial use, distribution, and reproduction in any medium, provided the original work is properly cited.


ORCID iDs

Saetbyul Hong 


<https://orcid.org/0000-0002-8185-9225>

Seung-Eun Lee 


<https://orcid.org/0000-0003-2353-8412>

Insung Kang 


<https://orcid.org/0000-0003-1792-5002>

Jehoon Yang 

<https://orcid.org/0000-0002-5808-9998>

Hunnyun Kim 

<https://orcid.org/0000-0003-1251-1994>

Jeyun Kim 

<https://orcid.org/0000-0003-0518-7022>

Kyung-Sun Kang 

<https://orcid.org/0000-0002-9322-741X>

## ABSTRACT

**Background:** Niemann-Pick disease type C (NPC) is caused by the mutation of *NPC* genes, which leads to the abnormal accumulation of unesterified cholesterol and glycolipids in lysosomes. This autosomal recessive disease is characterized by liver dysfunction, hepatosplenomegaly, and progressive neurodegeneration. Recently, the application of induced neural stem cells (iNSCs), converted from fibroblasts using specific transcription factors, to repair degenerated lesions has been considered a novel therapy.

**Objectives:** The therapeutic effects on NPC by human iNSCs generated by our research group have not yet been studied *in vivo*; in this study, we investigate those effects.

**Methods:** We used an NPC mouse model to efficiently evaluate the therapeutic effect of iNSCs, because neurodegeneration progress is rapid in NPC. In addition, application of human iNSCs from NPC patient-derived fibroblasts in an NPC model *in vivo* can give insight into the clinical usefulness of iNSC treatment. The iNSCs, generated from NPC patient-derived fibroblasts using the SOX2 and HMGA2 reprogramming factors, were transplanted by intracerebral injection into NPC mice.

**Results:** Transplantation of iNSCs showed positive results in survival and body weight change *in vivo*. Additionally, iNSC-treated mice showed improved learning and memory in behavior test results. Furthermore, through magnetic resonance imaging and histopathological assessments, we observed delayed neurodegeneration in NPC mouse brains.

**Conclusions:** iNSCs converted from patient-derived fibroblasts can become another choice of treatment for neurodegenerative diseases such as NPC.

**Keywords:** Neural stem cells; cell transplantation; Niemann-Pick disease type C; neurodegenerative diseases

## INTRODUCTION

Niemann-Pick disease type C (NPC) is an autosomal recessive, lysosomal storage disease that is fatal but rare and has an incidence between 1:100,000 and 1:150,000 in humans [1]. However, recent reports suggest that there may be a late-onset NPC phenotype with a markedly higher incidence, in the order of 1:20,000 to 1:39,000 [2]. Mutation of the *NPC1* gene is the

**Funding**

This work was supported by the National Research Foundation of Korea (NRF) grant funded by the Ministry of Science and ICT (MSIT) (No. 2018R1A2B3008483) and (No. 2020R1A4A4078907).

**Conflict of Interest**

The authors declare no conflicts of interest.

**Author Contributions**

Conceptualization: Hong SB, Kang IS; Data curation: Hong SB, Yang JH, Kim HN, Kim JY; Investigation: Hong SB, Lee SE, Yang JH, Kim HN, Kim JY; Methodology: Yang JH, Kim HN, Kim JY; Resources: Lee SE, Kang IS; Supervision: Kang KS; Writing - original draft: Hong SB; Writing - review & editing: Hong SB, Kang IS, Lee SE.

cause of 95% of NPC cases, whereas mutation of the *NPC2* gene occurs in only 4% of cases [3]. Mutations of these genes are related to abnormal endosomal-lysosomal trafficking, which results in excessive accumulation of lipids in the lysosomes of multiple tissues [4].

The age of onset of NPC varies from infancy to early adulthood, and it is difficult to diagnose although the disease commonly shows neurologic symptoms; moreover, the neurological manifestations ultimately result in death [2]. Currently, there is no curative therapy for NPC; rather, therapies focus on relieving clinical symptoms [5]. However, it has been reported that cell therapy is becoming a promising therapeutic approach for neurodegenerative disorders [6].

The methods for obtaining optimal induced neural stem cells (iNSCs) for application in the treatment of Huntington's disease have been described by other research groups, and their results suggest that iNSCs may also be used for such treatments [7,8]. Several study groups have shown that NSC-mediated regulation of neurotrophic support can form a potential therapy for various neurodegenerative disorders [9-12]. Most recently, several research groups demonstrated the direct conversion of fibroblasts into NSCs and showed the possibility of their therapeutic effects [13-17]. Moreover, our research group reported the generation of iNSCs from human NPC patient-derived fibroblasts by using only two reprogramming factors, SOX2 and HMGA2 [18].

Although NPC is a rare disease, it proceeds severely and fatally; therefore, research to develop new therapies for this neurodegenerative disease must continue. There have been no reports on the effect of iNSCs in NPC. Therefore, we decided to investigate NPC preclinically by using a disease model. Furthermore, amelioration of neurodegenerative conditions such as Alzheimer's disease, Parkinson's disease, and Huntington's disease is a research theme currently receiving widespread attention [19-21]. However, these neurodegenerative disorders are generally late-onset diseases, and their symptoms begin to manifest with increasing age; thus, modeling such diseases via animal models requires large amounts of time and high expenditures [22]. Conversely, an NPC model, which can be induced by a genetic disorder and is characterized by rapid deterioration, is very beneficial because the evaluation of newly developed therapies against neurodegeneration can be performed efficiently [23]. In addition, applying human iNSCs converted from NPC patient-derived fibroblasts in an *in vivo* NPC model can provide an opportunity to predict their clinical efficacy and safety in patients.

## MATERIALS AND METHODS

### Animals

NPC mice were purchased from Jackson Laboratories, USA. The BALB/cNctr-*Npc*<sup>1m1N/J</sup> mice (stock number 003092) were housed and experimented upon in the Animal Research and Imaging Center of Samsung Medical Center in accordance with the guidelines of Samsung Medical Center, which has been accredited by the Association for Assessment and Accreditation of Laboratory Animal Care International. The experimental protocols were approved by the Institutional Animal Care and Use Committee (approval No. 20170221001). Mice were bred and genotyped from genomic DNA isolated from tail snips using the polymerase chain reaction (PCR)-based protocols suggested by Jackson Laboratories, USA (<https://www.jax.org/strain/003092>). Mice were housed in individually ventilated cages (Thoren Caging Systems, USA), with autoclaved wood chips for bedding and *ad libitum* access to irradiated diets (PicoLab Rodent Diet 20; Labdiet, USA) and sterile water. The vivarium

was maintained on a 12-h light/dark cycle at a constant temperature ( $23 \pm 2^\circ\text{C}$ ) and humidity ( $50 \pm 10\%$ ). The study included four experimental groups: iNSC-transplanted *NPCI*<sup>-/-</sup> mice (n = 9); phosphate-buffered saline (PBS)-injected *NPCI*<sup>-/-</sup> mice (n = 9); fibroblast-transplanted *NPCI*<sup>-/-</sup> mice (n = 7); PBS-injected *NPCI*<sup>+/+</sup> mice (n = 7). We used only female mice in this study to avoid the effect of behavioral responses to opposite-sex odors.

### Culture of human fibroblast-derived neural stem cells

The iNSCs were established from human NPC patient-derived skin fibroblasts (GM03123, GM18453; Coriell Institute for Medical Research, USA) and were characterized in a previous study [18]. The pMX-SOX2 and pMX-HMGA2 retroviral constructs were transfected into 293 FT cells (Invitrogen, USA) to produce high viral titers using FuGENE 6 Transfection Reagents (Roche Diagnostics, USA) and the viral supernatants were collected and used to infect NPC patient-derived fibroblasts. The transduced fibroblasts were cultured in NSC maintenance medium (ReNcell NSC Maintenance Media; Millipore, USA) with basic fibroblast growth factor (bFGF; Sigma, USA) and epidermal growth factor (EGF; Sigma) added to induce neural stem cells. NSC-like colonies were picked and cultured under neurosphere conditions as attached cells on poly-L-ornithine- and fibronectin-coated dishes repeatedly to generate homogenous iNSCs. As reported previously, the iNSCs showed an NSC-like morphology and expressed NSC-specific markers such as PAX6 and NESTIN. Furthermore, the iNSCs demonstrated differentiation into neurons, astrocytes, and oligodendrocytes, indicating that the generated iNSCs could function as NSCs.

### Surgical transplantation of the iNSCs into *NPCI*<sup>-/-</sup> mice brains

Anesthesia was induced with 5% isoflurane and maintained with 2% isoflurane via a facial mask in *NPCI*<sup>-/-</sup> and *NPCI*<sup>+/+</sup> mice at 8 weeks of age. *NPCI*<sup>-/-</sup> mice were placed in a stereotaxic apparatus (Digital Stereotaxic Instrument with Fine Drive; MyNeurolab, USA), and  $10^5$  iNSCs in 2  $\mu\text{L}$  of cell suspension with PBS or only PBS were injected into the right brain unilaterally (iNSCs in *NPCI*<sup>-/-</sup>, n = 9; PBS in *NPCI*<sup>-/-</sup>, n = 9). The injection coordinates were 2.0 mm posterior and 1.4 mm lateral to the bregma, and at a depth of 2.0 mm. Additionally,  $10^5$  fibroblasts in 2  $\mu\text{L}$  of cell suspension were also injected into the same site of the *NPCI*<sup>-/-</sup> brains to compare their effects with those of iNSCs (fibroblasts in *NPCI*<sup>-/-</sup>, n = 7). Injection of an equal volume of PBS was used in normal wild-type *NPCI*<sup>+/+</sup> mice as a sham control (PBS in *NPCI*<sup>+/+</sup>, n = 7). After transplantation, the skin incised was closed by suture, and the mice were recovered from the anesthesia.

### Behavior tests

The Y-maze test and the fear conditioning test were performed at 10 weeks of age, two weeks after the transplantation of iNSCs, PBS, or fibroblasts. The spontaneous alternation Y-maze test was conducted to provide results indicative of spatial cognitive ability because mice typically prefer to investigate a new arm of a maze rather than returning to one that was previously visited. This is based on the natural tendency of rodents to explore a novel environment. In addition, for efficient alternation, mice need to use memory to recall which arm was previously visited. Therefore, a higher spontaneous alternation rate indicates a better working memory. A Y-shaped maze apparatus with three opaque plastic arms at angles of  $120^\circ$  from each other was used. The mice were placed in one arm of the maze and allowed to explore the three arms for 8 min. Spontaneous alternation performance was assessed by scoring the pattern of entries into each arm. The movements and number of entries to each arm were recorded using a video tracking system (Etho Vision XT 10; Noldus, Netherlands).

Mice behaviors were first recorded in the Y-maze with the fear conditioning test applied the next day to prevent the Y-maze test results from being affected by the fear test's aversive stimulus. The fear conditioning test was used to assess learning and memory ability as mice learn to associate neutral (tone) and aversive (mild electrical foot shock) stimuli, memorize those stimuli, and then respond, such as by freezing in the test chamber (Fear Conditioning System; Coulbourn Instruments, USA). On the first day, mice were placed in the fear conditioning system chamber and acclimated for 2 min to measure their “baseline” activity level. They then received a tone (80 dB, 3,600 Hz, 30 sec) followed by an aversive stimulus (0.2 mA, 2 sec), which ended with the tone. On the second day, the mice were placed in the same chamber, and their movements monitored without stimulation for 5 min (“contextual” fear conditioning). This approach allowed measurement of their ability to remember and association of the environment with the aversive stimulus. On the last day, mice were placed in a chamber with a new environment and acclimated to their surroundings for 2 min, followed by an identical tone as that on the first day (80 dB, 3,600 Hz, 180 sec) to allow “cued” fear conditioning to assess their memory associated with the acoustic tone and the aversive stimulus. A freezing response to the tone was defined as the complete lack of motion for a minimum of 0.75 sec. The freezing response percentages in each assessment period (i.e., during 2 min on the first day, during 5 min on the second day, and during the tones [180 sec] on the last day) were measured.

### Magnetic resonance imaging acquisition

Magnetic resonance imaging (MRI) of mouse brains was acquired at 10 weeks of age for each iNSC-treated *NPCI*<sup>-/-</sup> mouse and nontreated *NPCI*<sup>-/-</sup> mouse using a 7T/20 MRI System (Bruker-Biospin, Germany) equipped with a 20 cm gradient set capable of supplying up to 400 mT/m in a 100 μs rise time.

A quadrature birdcage coil (inner diameter of 72 mm; Bruker-Biospin, Germany) was used for excitation, and an actively decoupled phased array brain coil was used for signal reception. All mice were anesthetized under 2% isoflurane during MRI and their body temperatures were maintained at 36°C by using a heating pad. A T2-weighted spin-echo sequence was used during MRI scanning. The MRI parameters were: repetition time (TR)/echo time (TE) = 2,800/60 msec, number of averages = 16, echo train length = 8; in-plane resolution = 100 μm × 100 μm; slice thickness = 0.7 mm.

### Histologic analysis of brain tissue and tracking of transplanted iNSCs

The iNSC-treated *NPCI*<sup>-/-</sup> mice and nontreated *NPCI*<sup>-/-</sup> mice were sacrificed at 10 weeks of age to determine differences in brain tissues between the two groups. Each mouse was anesthetized by intraperitoneal injection of avertin (250 mg/kg) and then perfused with PBS, followed by a 4% paraformaldehyde fixative. Brains were removed and left in the fixative for 24 h, embedded in paraffin, and 4 μm coronal sections obtained. Sections were stained with hematoxylin and eosin for histologic examination under light microscopy.

To track the injected human iNSCs in the brain of *NPCI*<sup>-/-</sup> mice, immunohistochemical analysis was performed. Deparaffinized tissue sections were blocked with mouse IgG (MOM, Vector, USA) and incubated with anti-human mitochondria mouse IgG (1:400, MAB1273; Millipore, USA) for 60 min at room temperature in a humidified dark chamber. Then, the sections were incubated with Alexa Fluor 594 goat anti-mouse secondary antibody. Nuclei were counterstained with DAPI. Stained images were observed under light and fluorescence microscopy (BX53; Olympus, Japan).

### Statistical analysis

The data were compared by applying one-way analysis of variance followed by Student's *t*-test. A value of  $p < 0.05$  was considered statistically significant. All values are expressed as a mean  $\pm$  standard deviation.

## RESULTS

### iNSC treatment delayed body weight loss and extended the life span of *NPCT*<sup>-/-</sup> mice

The body weights and clinical signs of *NPCT*<sup>-/-</sup> mice were observed from 4 weeks of age. The *NPCT*<sup>-/-</sup> mice experienced growth stagnation and abnormal clinical signs, such as tremors, from 7 weeks of age compared to those of *NPCT*<sup>+/+</sup> mice. The NPC-iNSCs were transplanted into the brains of *NPCT*<sup>-/-</sup> mice at 8 weeks of age. To compare effects, PBS or NPC-fibroblasts were transplanted into the same positions in the brains of *NPCT*<sup>-/-</sup> mice. The iNSC-treated *NPCT*<sup>-/-</sup> mice showed delayed weight loss and a longer survival period than those in nontreated *NPCT*<sup>-/-</sup> mice or fibroblast-treated *NPCT*<sup>-/-</sup> mice. In particular, at 10 weeks of age, nontreated *NPCT*<sup>-/-</sup> mice and fibroblast-treated *NPCT*<sup>-/-</sup> mice showed significant weight loss. In contrast, iNSC-treated *NPCT*<sup>-/-</sup> mice showed less weight reduction at 10 weeks of age but exhibited significant weight loss at 11 weeks of age (iNSC-injected *NPCT*<sup>-/-</sup> 14.00  $\pm$  0.82 g; PBS-injected *NPCT*<sup>-/-</sup> 11.57  $\pm$  1.13 g; fibroblast-injected *NPCT*<sup>-/-</sup> 11.86  $\pm$  1.35 g at 10 weeks) ( $p < 0.01$ ) (**Fig. 1**).

### iNSC treatment enhanced learning and memory in *NPCT*<sup>-/-</sup> mice

The iNSC-treated *NPCT*<sup>-/-</sup> mice showed a longer fear response (freezing period), compared to that in the PBS and fibroblast-treated *NPCT*<sup>-/-</sup> mice in the fear conditioning test (iNSC-injected *NPCT*<sup>-/-</sup> 52.28  $\pm$  3.92 sec; PBS-injected *NPCT*<sup>-/-</sup> 10.83  $\pm$  4.15 sec; fibroblast-injected *NPCT*<sup>-/-</sup> 25.09  $\pm$  7.50 sec) ( $p < 0.001$  between iNSC- and PBS-injected groups,  $p < 0.05$  between iNSC- and fibroblast-injected groups) (**Fig. 2B**). The results indicate that iNSC-treated *NPCT*<sup>-/-</sup> mice exhibited enhanced learning and memory related to the tone and mild electrical shock stimuli. In the Y-maze test, iNSC-treated *NPCT*<sup>-/-</sup> mice showed a greater preference for the

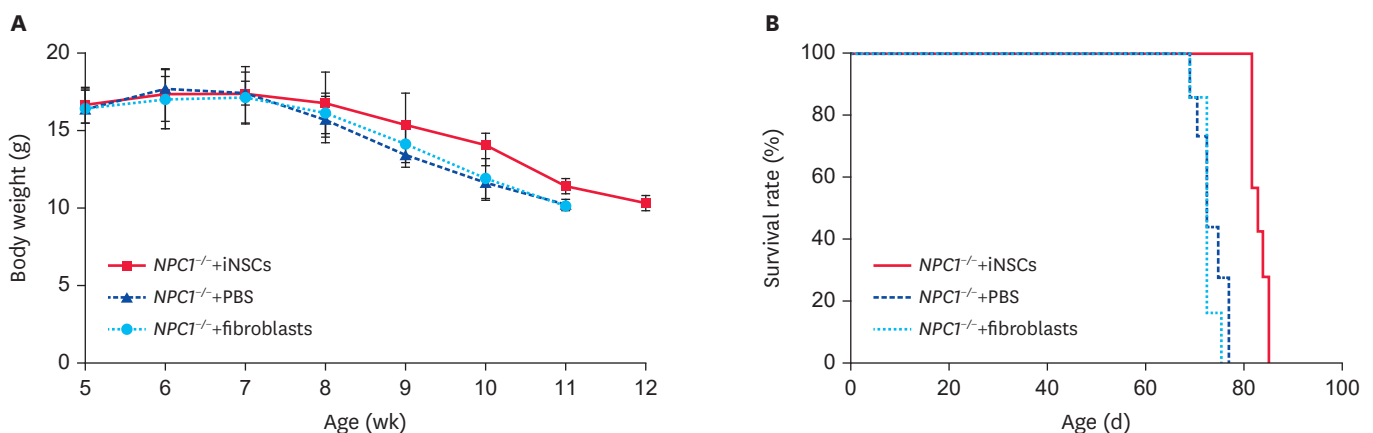


**Fig. 1.** Body weight loss of *NPCT*<sup>-/-</sup> mice laterally injected with iNSCs in the brain (2.0 mm posterior and 1.4 mm lateral to bregma and at a depth of 2.0 mm) with human iNSCs ( $n = 9$ ), PBS ( $n = 9$ ), or human fibroblasts ( $n = 7$ ). iNSC-injected *NPCT*<sup>-/-</sup> mice displayed significantly less weight loss than the PBS- or fibroblast-injected groups ( $p < 0.01$ ) at 10 weeks (A). Life spans were observed to determine the survival rate of *NPCT*<sup>-/-</sup> mice and assess the effectiveness of human iNSCs ( $n = 9$ ), PBS ( $n = 9$ ), and fibroblast ( $n = 7$ ) injections. iNSC-injected mice survived longer than PBS- or fibroblast-injected mice (iNSCs 83  $\pm$  2 days, PBS 74  $\pm$  3 days, fibroblasts 73  $\pm$  1 days) ( $p < 0.001$ ).

NPCT, Niemann-Pick disease type C; iNSC, induced neural stem cell; PBS, phosphate-buffered saline.

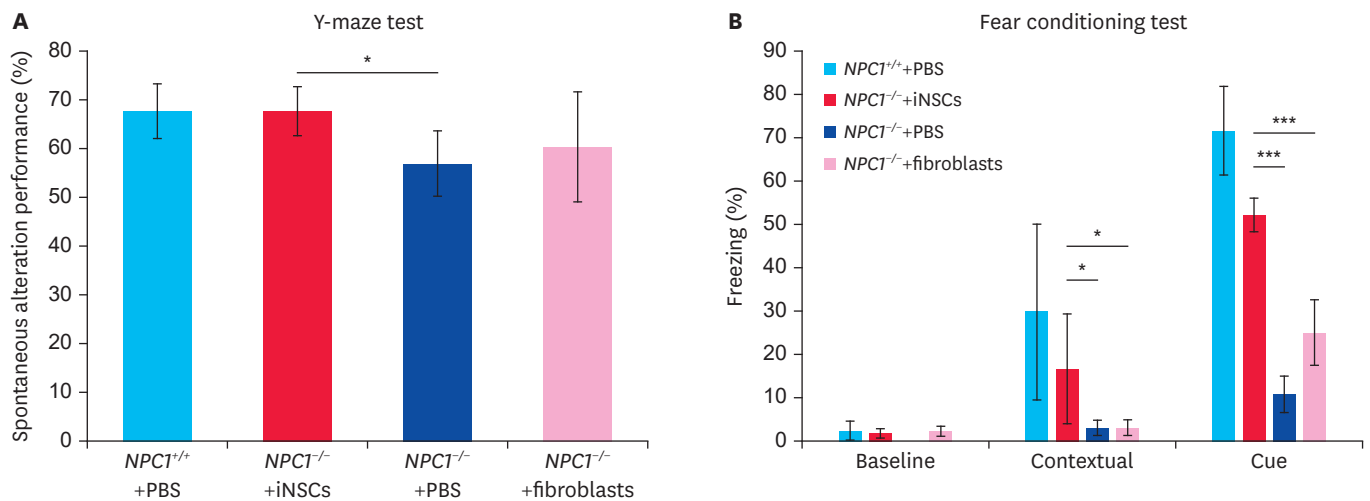


**Fig. 2.** Behavior test results of NPC mice treated with human iNSCs ( $n = 5$ ), PBS ( $n = 5$ ), or human fibroblasts ( $n = 5$ ). Compared to the PBS-injected mice, the iNSC-injected *NPC1*<sup>-/-</sup> mice displayed a greater preference for the new arm in the Y-maze at the age of 10 weeks ( $p < 0.05$ ) (A). In the fear conditioning test, iNSC-injected *NPC1*<sup>-/-</sup> mice had a longer freezing response than that of PBS- or fibroblast-treated mice for both contextual fear conditioning ( $p < 0.05$ ) and cued fear conditioning ( $p < 0.001$ ) (B).

NPC, Niemann-Pick disease type C; iNSC, induced neural stem cell; PBS, phosphate-buffered saline.

new arm of the maze compared to that of the PBS- and fibroblast-treated *NPC1*<sup>-/-</sup> mice. The iNSC-injected *NPC1*<sup>-/-</sup> mice displayed a spontaneous alternation rate of  $68 \pm 5\%$ , significantly higher than the  $57.2 \pm 6.9\%$  spontaneous alternation rate for the PBS-injected *NPC1*<sup>-/-</sup> mouse group ( $p < 0.001$  between the iNSC- and PBS-injected groups) (Fig. 2A).

### iNSC treatment delayed degeneration of the brains of *NPC1*<sup>-/-</sup> mice

We compared the brains of a single *NPC1*<sup>-/-</sup> mouse, one iNSC-treated mouse, and one nontreated mouse to assess differences in the cross-sectional areas in T2-weighted images and determine if there were treatment related side effects. The overall brain size of the iNSC-treated *NPC1*<sup>-/-</sup> mouse was larger than that of the nontreated *NPC1*<sup>-/-</sup> mouse based on the T2-weighted images from MRI scanning obtained at 10 weeks of age. The specified cross-sectional area of the single nontreated *NPC1*<sup>-/-</sup> mouse brain was compared to that of the iNSC-treated mouse (Supplementary Fig. 1). The areas were measured with the help of ImageJ image analysis software. Additionally, there were no signs of side effects (e.g., tumor or inflammation) related to the injection of iNSCs.

Histological analysis revealed that the total size of the brains of nontreated *NPC1*<sup>-/-</sup> mice was substantially smaller than that of iNSC-treated *NPC1*<sup>-/-</sup> mice at 10 weeks of age (2 weeks after transplantation). In particular, neuron loss in the thalamus of the nontreated *NPC1*<sup>-/-</sup> mice was much greater than that in the iNSC-treated *NPC1*<sup>-/-</sup> mice. The neuronal cells of the iNSC-treated *NPC1*<sup>-/-</sup> mice, especially in certain damaged parts of the brain, seem to have been protected from disease progression by the treatment (Fig. 3).

### iNSCs were detected in transplanted *NPC1*<sup>-/-</sup> mice

The iNSCs injected 2.0 mm posterior and 1.4 mm lateral to the bregma and at a 2.0 mm depth were detected in the ventricle adjacent to the hippocampus of *NPC1*<sup>-/-</sup> mice at 2 days after transplantation. Fluorescently labeled iNSCs were observed, and immunohistochemical staining for human mitochondria revealed the location of the transplanted iNSCs (Fig. 4).

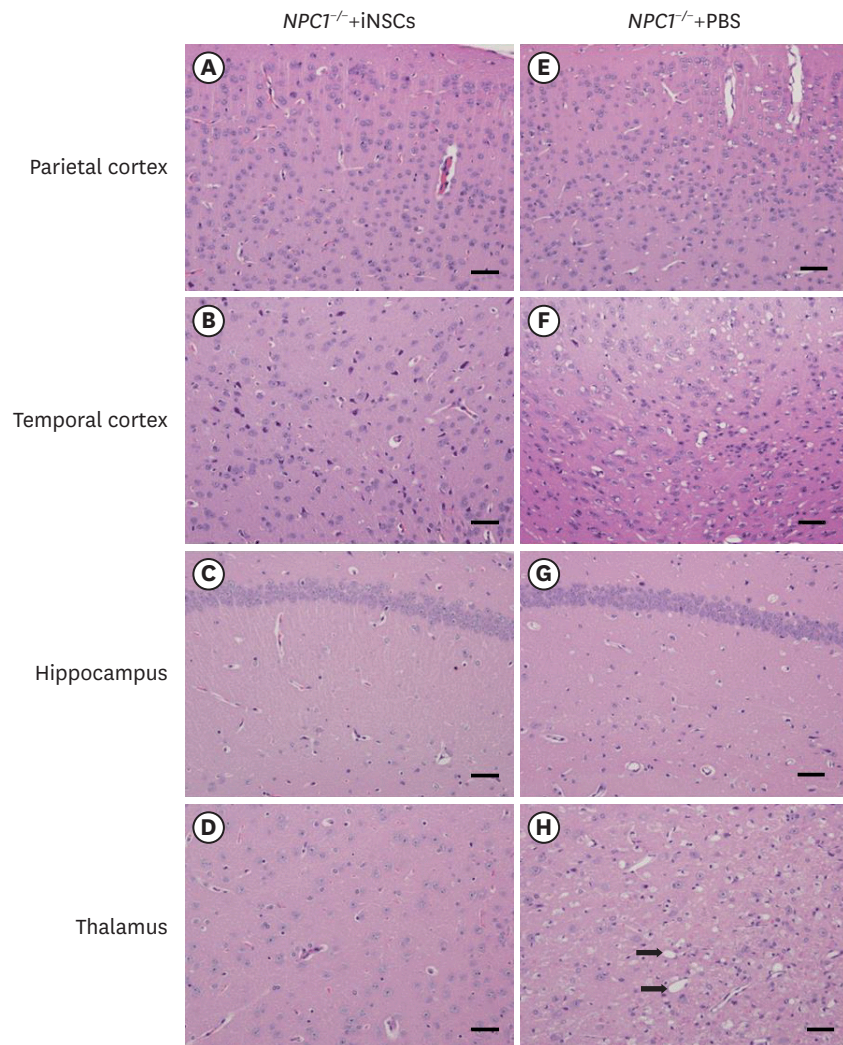


**Fig. 3.** Specific regions of hematoxylin & eosin stained brain from iNSC-treated  $NPC1^{-/-}$  (A, B, C, D) and nontreated  $NPC1^{-/-}$  mice (E, F, G, H) were compared. Brain areas examined included the parietal cortex, temporal cortex, hippocampus, and thalamus. The thalamus area of iNSC-treated  $NPC1^{-/-}$  mice exhibited significantly less deterioration than the same area of untreated  $NPC1^{-/-}$  mice (D, H). Untreated  $NPC1^{-/-}$  mice showed prominently visible vacuolation (arrows) and neuronal degeneration (200 $\times$  magnification, scale bar = 50  $\mu$ m). iNSC, induced neural stem cell; NPC, Niemann-Pick disease type C; PBS, phosphate-buffered saline.

The injected cells remained in the brains of the treated mice for several days and appear to have contributed to a delay in the neurodegeneration in the treated  $NPC1^{-/-}$  mice.

## DISCUSSION

The inherited lysosomal storage disease NPC presents with signs of progressive neurodegeneration such as cognitive decline and mental retardation. To reveal the effects of an iNSCs treatment on this neurodegenerative disease, we transplanted iNSCs into the brains of  $NPC1^{-/-}$  mice, evaluated neurodegenerative symptoms and behavioral signs, and compared the results to those from nontreated  $NPC1^{-/-}$  mice.

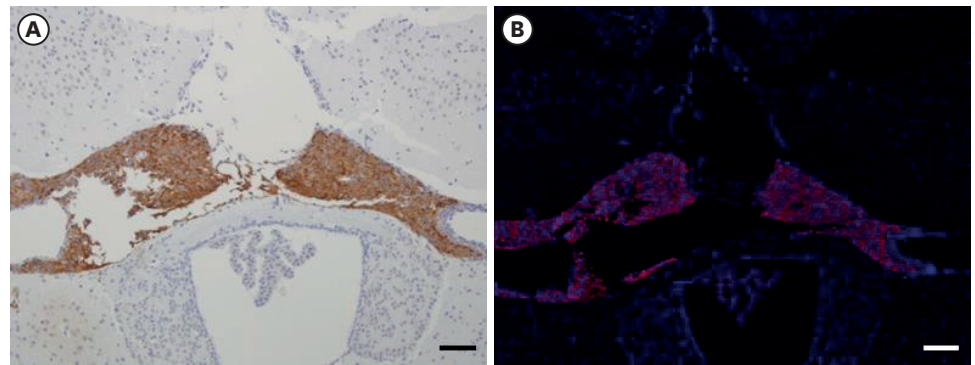


**Fig. 4.** Immunohistochemical staining of the brain of a 10-week-old *NPC1*<sup>-/-</sup> mouse that received a stereotactic injection of human iNSCs into a region 2.0 mm posterior and 1.4 mm lateral to the bregma, and at a depth of 2.0 mm. Anti-human mitochondrial mouse IgG (1:400 dilution) detected injected human iNSC clusters (A). Immunofluorescent images identifying human iNSCs (red) and cell nuclei with DAPI (blue) (B) (100× magnification, scale bar = 100 µm). NPC, Niemann-Pick disease type C; iNSC, induced neural stem cell; IgG, immunoglobulin G; DAPI, 4',6-diamidino-2-phenylindole.

Recently, several groups have reported on converting somatic cells directly into iNSCs by using specific transcription factors. Among them, reprogramming of fibroblasts is relatively newly reported [24-27]. Other research groups have tried to verify the efficacy of therapeutic transplantation in various disease models [13-17]. The generation of iNSCs from fibroblasts has several advantages because fibroblasts are easier to obtain than other somatic cell types. Once obtained, iNSCs are expected to self-renew and differentiate to multiple neuronal subtypes and glial cells. In addition, iNSCs are associated with a lower risk of teratoma formation, and they can be suitable for clinical application via autologous transplantation [7]. Such treatments can be quickly developed to allow their use before the effects of the disease become irreparable due to their rapid and direct induction [28].

In a previous study, our research group described the direct reprogramming of NPC patient-derived fibroblasts into iNSCs by using 2 reprogramming factors, SOX2 and HMG2 [18]. These iNSCs exhibited an NSC-like morphology, clearly different from that of human fibroblasts. They also expressed NSC markers such as PAX6 and NESTIN. Although there have been many studies into the development of variable iNSCs, this present study was the first to generate human iNSCs from a patient with NPC. Based on this study, it is possible to test the potential for patient therapy by an approach that incorporates the patient's converted iNSCs into a model of the same disease. *In vivo* testing that uses patient-derived converted iNSCs could provide insight into the potential of iNSCs for therapeutic use. Although NPC patient-derived fibroblasts may have genetic problems, we decided to utilize these cells to obtain insight in the clinical usefulness of iNSC treatment using a patient-specific tissue. The ideal way to determine that usefulness is through the transplantation of genetically corrected iNSCs into NPC human patients, but such a clinical trial is impossible in reality. Moreover, inducing genetic correction of patient-derived cells into neural stem cells is a significant challenge. Therefore, in this study, we chose to investigate this use of iNSCs in an NPC mice model. Even though it is doubtful these iNSCs contained "corrected" genetic mutations of the *NPC1* gene, we hypothesized that the generated and transplanted iNSCs could induce the positive effect of attenuating neurodegeneration via neurotrophic effects. We are also interested in the challenge of accomplishing the correction of mutated *NPC1* genes and the generation of corrected neural stem cells.



The *NPCI*<sup>+/−</sup> NPC disease model mice began to lose weight and show neurodegenerative signs such as tremors from 7 weeks of age. In a real clinical situation, neurodegenerative disorders have heterogeneous presentation timing, and diagnostic accuracy is difficult; therefore, attempts at treatment can occur after clinical signs are presented [29]. Therefore, we attempted to determine the effects of transplanted iNSCs on symptom expression in the model. Even though the study included xenotransplantation we did not use an immune-suppressant. Other researchers indicated there is a possibility of significant dysregulation of innate immunity in NPC [30]. Furthermore, the brain and central nervous system are separate from the body's immune system, forming the “neuroimmune system,” with the brain exhibiting a less hostile immune response than other parts of the body and may be considered as ‘immunologically privileged’ [31]. Based on these research opinions, we assumed that the injection of an immunosuppressant to the body via intravenous or subcutaneous routes would not affect the neuroimmune system, and we decided to undertake this study without using an immunosuppressant. We transplanted the iNSCs into the brains of *NPCI*<sup>+/−</sup> mice at the age of 8 weeks and monitored their responses. The mice were given two weeks to recover from the stereotaxic surgery and at 10 weeks of age, we performed behavioral, MRI, and histological assessments to compare treated and nontreated groups. The results indicated that iNSC-transplanted *NPCI*<sup>+/−</sup> mice had less body weight loss and survived longer than nontreated *NPCI*<sup>+/−</sup> mice. In particular, at 10 weeks of age (2 weeks after transplantation), there was a marked difference in body weights of the 2 groups (2.43 g). Considering the average body weight of *NPCI*<sup>+/−</sup> mice at 10 weeks of age was 11.57 g, the difference was significant. Although such a conclusion is tenuous, we assume that iNSC transplantation is effective *in vivo* for at least 2 weeks. In the clinical treatment of other neurodegenerative diseases, sustained improvements can be expected when repetitive cell transplantations are provided [32,33]. *NPCI*<sup>+/−</sup> mice are characterized by rapid deterioration and early death. Therefore, we were unable to undertake long-term research with the NPC disease model mice. Moreover, our research scheme involved treatment after identifying clinically abnormal symptoms. Thus, we could only obtain 2 weeks of post-transplant data. To assess iNSC treatment efficacy over a longer term, we think other models of neurodegenerative disorders should be investigated.

We also decided to assess the behaviors of iNSC-treated *NPCI*<sup>+/−</sup> mice, particularly to investigate their recognition, learning, and memory abilities. We observed remarkable differences between groups in performance in the fear conditioning test compared to those in the Y-maze test. The iNSC-treated *NPCI*<sup>+/−</sup> mice learned and memorized the stimuli offered in the fear conditioning test by expressing the freezing fear response more than that by nontreated *NPCI*<sup>+/−</sup> mice. Additionally, our MRI and histopathological observations provided insights into degenerative differences between iNSC-treated and nontreated mice.

We undertook to verify the presence of injected cells at 48 h after transplantation because we predicted that the transplanted human iNSCs would leave the injection site within a short time and migrate into other sites. However, detection of iNSCs at sequential time-points after implantation, such as undertaken by other research teams [34,35], was not performed.

According to the MRI and histopathological results, the overall brain size of iNSC-treated *NPCI*<sup>+/−</sup> mice was larger than that of nontreated *NPCI*<sup>+/−</sup> mice. Overall, atrophy of the *NPCI*<sup>+/−</sup> brain is apparent, with significantly reduced volumes detected in the striatum, thalamus, and cortex, as reported by another research group [36,37]. Furthermore, it has been revealed that neurological phenotypes displayed by *NPCI*<sup>+/−</sup> mice include widespread activation of astrocytes and microglia, particularly in the thalamus [38-42]. We observed significant neuronal loss, especially in the thalamus, in nontreated *NPCI*<sup>+/−</sup> mice, as has been previously reported.

Conversely, the iNSC-transplanted *NPCI*<sup>-/-</sup> mouse thalamus showed comparatively less neuronal cell loss and less size loss. Our results and those of previous investigators suggest that the brain, especially the thalamus, of *NPCI*<sup>-/-</sup> mice may be protected by the transplantation of iNSCs, which has the effect of delaying neurodegeneration. Studies have shown that iNSCs can protect against cell death caused by inflammation through COX-2 regulation or inhibition of neuronal apoptosis [43,44]. Another recent study showed that transplanted iNSCs exert neurotrophic effects, such as upregulation of brain-derived neurotrophic factor (BDNF) and glial-derived neurotrophic factor, in addition to decreased immune cell recruitment and pro-inflammatory cytokine expression in the damaged brain [16]. Previous studies have demonstrated the neuroprotective features of iNSCs. In the past, studies of NSC transplantation have focused on assessing the replacement of dying cells, but many study groups now suggest that transplanted stem cells are active in neurogenesis and improve cognitive function due to an elevation in the expression of neurotrophins such as BDNF and nerve growth factor [9,11,45].

Previously, the thalamus was viewed as a passive structure; however, in recent years, it has been revealed that the thalamus has a central role in cognition, ranging from learning and memory to flexible adaptation [46,47]. In our experiment, we observed the greatest histopathological difference between iNSC-treated *NPCI*<sup>-/-</sup> mice and nontreated *NPCI*<sup>-/-</sup> mice in the thalamus. Among the various brain regions, the thalamus is the part of *NPCI*<sup>-/-</sup> mice brain that presents the most severe progression of the disease, including vacuolation. Based on previous reports and our results, we assume that differences between degenerated and protected thalamic regions can affect cognition, learning, and memory in *NPCI*<sup>-/-</sup> mice.

Reprogramming of fibroblasts into iNSCs can be a potentially unlimited source of neurons and the use of iNSCs can avoid the risk of teratoma formation and ethical issues. The application of iNSCs to the brain, by its capacity to induce the expressions of neurotrophin and anti-inflammatory factors, may be an effective method to reduce neuronal loss in various brain diseases. Further studies into NSC modeling and related mechanisms could provide additional indications of the therapeutic potential of iNSCs in future clinical use.

## ACKNOWLEDGMENTS

We would like to thank the Animal Research and Molecular Imaging Center of Samsung Medical Center for participation in this study.

## SUPPLEMENTARY MATERIAL

### Supplementary Fig. 1

T2-weighted MRI *in vivo* image and hematoxylin & eosin staining of brains from iNSC-treated *NPCI*<sup>-/-</sup> and nontreated *NPCI*<sup>-/-</sup> mouse at 10 weeks of age. The brain of the nontreated *NPCI*<sup>-/-</sup> mouse (B) appears reduced in size relative to the iNSC-treated *NPCI*<sup>-/-</sup> mouse (A). Upon specifically comparing the images in the blue squares, the cross-sectional brain area of the nontreated *NPCI*<sup>-/-</sup> mouse (n = 1) was 87.2% of iNSC-treated mouse (n = 1) brain region (A, B). Histological comparison reveals that atrophy of the nontreated *NPCI*<sup>-/-</sup> mouse brain was apparent compared to the iNSC-treated mouse brain (C, D).

[Click here to view](#)

## REFERENCES

1. Vanier MT. Niemann-Pick disease type C. *Orphanet J Rare Dis.* 2010;5(1):16.  
[PUBMED](#) | [CROSSREF](#)
2. Wassif CA, Cross JL, Iben J, Sanchez-Pulido L, Cougnoux A, Platt FM, Ory DS, Ponting CP, Bailey-Wilson JE, Biesecker LG, Porter FD. High incidence of unrecognized visceral/neurological late-onset Niemann-Pick disease, type C1, predicted by analysis of massively parallel sequencing data sets. *Genet Med.* 2016;18(1):41-48.  
[PUBMED](#) | [CROSSREF](#)
3. Pineda M, Walterfang M, Patterson MC. Miglustat in Niemann-Pick disease type C patients: a review. *Orphanet J Rare Dis.* 2018;13(1):140.  
[PUBMED](#) | [CROSSREF](#)
4. Vanier MT. Complex lipid trafficking in Niemann-Pick disease type C. *J Inher Metab Dis.* 2015;38(1):187-199.  
[PUBMED](#) | [CROSSREF](#)
5. Geberhiwot T, Moro A, Dardis A, Ramaswami U, Sirrs S, Marfa MP, Vanier MT, Walterfang M, Bolton S, Dawson C, Héron B, Stampfer M, Imrie J, Hendriks C, Gissen P, Crushell E, Coll MJ, Nadjar Y, Klünemann H, Mengel E, Hrebicek M, Jones SA, Ory D, Bembi B, Patterson M International Niemann-Pick Disease Registry (INPDR). Consensus clinical management guidelines for Niemann-Pick disease type C. *Orphanet J Rare Dis.* 2018;13(1):50.  
[PUBMED](#) | [CROSSREF](#)
6. Tang Y, Yu P, Cheng L. Current progress in the derivation and therapeutic application of neural stem cells. *Cell Death Dis.* 2017;8(10):e3108.  
[PUBMED](#) | [CROSSREF](#)
7. Choi KA, Hong S. Induced neural stem cells as a means of treatment in Huntington's disease. *Expert Opin Biol Ther.* 2017;17(11):1333-1343.  
[PUBMED](#) | [CROSSREF](#)
8. Choi KA, Choi Y, Hong S. Stem cell transplantation for Huntington's diseases. *Methods.* 2018;133:104-112.  
[PUBMED](#) | [CROSSREF](#)
9. Marsh SE, Blurton-Jones M. Neural stem cell therapy for neurodegenerative disorders: the role of neurotrophic support. *Neurochem Int.* 2017;106:94-100.  
[PUBMED](#) | [CROSSREF](#)
10. Goldberg NRS, Caesar J, Park A, Sedgh S, Finogenov G, Masliah E, Davis J, Blurton-Jones M. Neural stem cells rescue cognitive and motor dysfunction in a transgenic model of dementia with Lewy bodies through a BDNF-dependent mechanism. *Stem Cell Reports.* 2015;5(5):791-804.  
[PUBMED](#) | [CROSSREF](#)
11. Blurton-Jones M, Kitazawa M, Martinez-Coria H, Castello NA, Müller FJ, Loring JF, Yamasaki TR, Poon WW, Green KN, LaFerla FM. Neural stem cells improve cognition via BDNF in a transgenic model of Alzheimer disease. *Proc Natl Acad Sci U S A.* 2009;106(32):13594-13599.  
[PUBMED](#) | [CROSSREF](#)
12. Carletti B, Piemonte F, Rossi F. Neuroprotection: the emerging concept of restorative neural stem cell biology for the treatment of neurodegenerative diseases. *Curr Neuropharmacol.* 2011;9(2):313-317.  
[PUBMED](#) | [CROSSREF](#)
13. Choi DH, Kim JH, Kim SM, Kang K, Han DW, Lee J. Therapeutic potential of induced neural stem cells for Parkinson's disease. *Int J Mol Sci.* 2017;18(1):224.  
[PUBMED](#) | [CROSSREF](#)
14. Yamashita T, Liu W, Matsumura Y, Miyagi R, Zhai Y, Kusaki M, Hishikawa N, Ohta Y, Kim SM, Kwak TH, Han DW, Abe K. Novel therapeutic transplantation of induced neural stem cells for stroke. *Cell Transplant.* 2017;26(3):461-467.  
[PUBMED](#) | [CROSSREF](#)
15. Hemmer K, Zhang M, van Wüllen T, Sakalem M, Tapia N, Baumuratov A, Kaltschmidt C, Kaltschmidt B, Schöler HR, Zhang W, Schwamborn JC. Induced neural stem cells achieve long-term survival and functional integration in the adult mouse brain. *Stem Cell Reports.* 2014;3(3):423-431.  
[PUBMED](#) | [CROSSREF](#)
16. Gao M, Yao H, Dong Q, Zhang Y, Yang Y, Zhang Y, Yang Z, Xu M, Xu R. Neurotrophin and immunomodulation of induced neural stem cell grafts in a mouse model of closed head injury. *Stem Cell Res (Amst).* 2017;23:132-142.  
[PUBMED](#) | [CROSSREF](#)
17. Xie C, Liu YQ, Guan YT, Zhang GX. Induced stem cells as a novel multiple sclerosis therapy. *Curr Stem Cell Res Ther.* 2016;11(4):313-320.  
[PUBMED](#) | [CROSSREF](#)

18. Sung EA, Yu KR, Shin JH, Seo Y, Kim HS, Koog MG, Kang I, Kim JJ, Lee BC, Shin TH, Lee JY, Lee S, Kang TW, Choi SW, Kang KS. Generation of patient specific human neural stem cells from Niemann-Pick disease type C patient-derived fibroblasts. *Oncotarget*. 2017;8(49):85428-85441.  
[PUBMED](#) | [CROSSREF](#)
19. Duncan T, Valenzuela M. Alzheimer's disease, dementia, and stem cell therapy. *Stem Cell Res Ther*. 2017;8(1):111.  
[PUBMED](#) | [CROSSREF](#)
20. Napoli E, Borlongan CV. Cell therapy in Parkinson's disease: host brain repair machinery gets a boost from stem cell grafts. *Stem Cells*. 2017;35(6):1443-1445.  
[PUBMED](#) | [CROSSREF](#)
21. Fink KD, Deng P, Torrest A, Stewart H, Pollock K, Gruenloh W, Annett G, Tempkin T, Wheelock V, Nolte JA. Developing stem cell therapies for juvenile and adult-onset Huntington's disease. *Regen Med*. 2015;10(5):623-646.  
[PUBMED](#) | [CROSSREF](#)
22. Singh S, Srivastava A, Srivastava P, Dhuriya YK, Pandey A, Kumar D, Rajpurohit CS. Advances in stem cell research- a ray of hope in better diagnosis and prognosis in neurodegenerative diseases. *Front Mol Biosci*. 2016;3:72.  
[PUBMED](#) | [CROSSREF](#)
23. German DC, Liang CL, Song T, Yazdani U, Xie C, Dietschy JM. Neurodegeneration in the Niemann-Pick C mouse: glial involvement. *Neuroscience*. 2002;109(3):437-450.  
[PUBMED](#) | [CROSSREF](#)
24. Han DW, Tapia N, Hermann A, Hemmer K, Höing S, Araúzo-Bravo MJ, Zaehres H, Wu G, Frank S, Moritz S, Greber B, Yang JH, Lee HT, Schwamborn JC, Storch A, Schöler HR. Direct reprogramming of fibroblasts into neural stem cells by defined factors. *Cell Stem Cell*. 2012;10(4):465-472.  
[PUBMED](#) | [CROSSREF](#)
25. Thier M, Wörsdörfer P, Lakes YB, Gorris R, Herms S, Opitz T, Seiferling D, Quandel T, Hoffmann P, Nöthen MM, Brüstle O, Edenhofer F. Direct conversion of fibroblasts into stably expandable neural stem cells. *Cell Stem Cell*. 2012;10(4):473-479.  
[PUBMED](#) | [CROSSREF](#)
26. Zhang M, Lin YH, Sun YJ, Zhu S, Zheng J, Liu K, Cao N, Li K, Huang Y, Ding S. Pharmacological reprogramming of fibroblasts into neural stem cells by signaling-directed transcriptional activation. *Cell Stem Cell*. 2016;18(5):653-667.  
[PUBMED](#) | [CROSSREF](#)
27. Yu KR, Shin JH, Kim JJ, Koog MG, Lee JY, Choi SW, Kim HS, Seo Y, Lee S, Shin TH, Jee MK, Kim DW, Jung SJ, Shin S, Han DW, Kang KS. Rapid and efficient direct conversion of human adult somatic cells into neural stem cells by HMGA2/let-7b. *Cell Reports*. 2015;10(3):441-452.  
[PUBMED](#) | [CROSSREF](#)
28. Goldman SA. Stem and progenitor cell-based therapy of the central nervous system: hopes, hype, and wishful thinking. *Cell Stem Cell*. 2016;18(2):174-188.  
[PUBMED](#) | [CROSSREF](#)
29. Erkkinen MG, Kim MO, Geschwind MD. Clinical neurology and epidemiology of the major neurodegenerative diseases. *Cold Spring Harb Perspect Biol*. 2018;10(4):a033118.  
[PUBMED](#) | [CROSSREF](#)
30. Platt N, Speak AO, Colaco A, Gray J, Smith DA, Williams IM, Wallom KL, Platt FM. Immune dysfunction in Niemann-Pick disease type C. *J Neurochem*. 2016;136 Suppl 1:74-80.  
[PUBMED](#) | [CROSSREF](#)
31. Louveau A, Harris TH, Kipnis J. Revisiting the mechanisms of CNS immune privilege. *Trends Immunol*. 2015;36(10):569-577.  
[PUBMED](#) | [CROSSREF](#)
32. Baek W, Kim YS, Koh SH, Lim SW, Kim HY, Yi HJ, Kim H. Stem cell transplantation into the intraventricular space via an Ommaya reservoir in a patient with amyotrophic lateral sclerosis. *J Neurosurg Sci*. 2012;56(3):261-263.  
[PUBMED](#)
33. Cizkova D, Novotna I, Slovinska L, Vanicky I, Jergova S, Rosocha J, Radonak J. Repetitive intrathecal catheter delivery of bone marrow mesenchymal stromal cells improves functional recovery in a rat model of contusive spinal cord injury. *J Neurotrauma*. 2011;28(9):1951-1961.  
[PUBMED](#) | [CROSSREF](#)
34. Magnitsky S, Watson DJ, Walton RM, Pickup S, Bulte JW, Wolfe JH, Poptani H. *In vivo* and *ex vivo* MRI detection of localized and disseminated neural stem cell grafts in the mouse brain. *Neuroimage*. 2005;26(3):744-754.  
[PUBMED](#) | [CROSSREF](#)

35. Wang Y, Xu F, Zhang C, Lei D, Tang Y, Xu H, Zhang Z, Lu H, Du X, Yang GY. High MR sensitive fluorescent magnetite nanocluster for stem cell tracking in ischemic mouse brain. *Nanomedicine (Lond)*. 2011;7(6):1009-1019.  
[PUBMED](#) | [CROSSREF](#)
36. Pressey SN, Smith DA, Wong AM, Platt FM, Cooper JD. Early glial activation, synaptic changes and axonal pathology in the thalamocortical system of Niemann-Pick type C1 mice. *Neurobiol Dis*. 2012;45(3):1086-1100.  
[PUBMED](#) | [CROSSREF](#)
37. Walterfang M, Patenaude B, Abel LA, Klunemann H, Bowman EA, Fahey MC, Desmond P, Kelso W, Velakoulis D. Subcortical volumetric reductions in adult Niemann-Pick disease type C: a cross-sectional study. *AJNR Am J Neuroradiol*. 2013;34(7):1334-1340.  
[PUBMED](#) | [CROSSREF](#)
38. Smith D, Wallom KL, Williams IM, Jeyakumar M, Platt FM. Beneficial effects of anti-inflammatory therapy in a mouse model of Niemann-Pick disease type C1. *Neurobiol Dis*. 2009;36(2):242-251.  
[PUBMED](#) | [CROSSREF](#)
39. Ahmad I, Lope-Piedrafita S, Bi X, Hicks C, Yao Y, Yu C, Chaitkin E, Howison CM, Weberg L, Trouard TP, Erickson RP. Allopregnanolone treatment, both as a single injection or repetitively, delays demyelination and enhances survival of Niemann-Pick C mice. *J Neurosci Res*. 2005;82(6):811-821.  
[PUBMED](#) | [CROSSREF](#)
40. Cougnoux A, Drummond RA, Collar AL, Iben JR, Salman A, Westgarth H, Wassif CA, Cawley NX, Farhat NY, Ozato K, Lionakis MS, Porter FD. Microglia activation in Niemann-Pick disease, type C1 is amendable to therapeutic intervention. *Hum Mol Genet*. 2018;27(12):2076-2089.  
[PUBMED](#) | [CROSSREF](#)
41. Baudry M, Yao Y, Simmons D, Liu J, Bi X. Postnatal development of inflammation in a murine model of Niemann-Pick type C disease: immunohistochemical observations of microglia and astroglia. *Exp Neurol*. 2003;184(2):887-903.  
[PUBMED](#) | [CROSSREF](#)
42. Yamada A, Saji M, Ukita Y, Shinoda Y, Taniguchi M, Higaki K, Ninomiya H, Ohno K. Progressive neuronal loss in the ventral posterior lateral and medial nuclei of thalamus in Niemann-Pick disease type C mouse brain. *Brain Dev*. 2001;23(5):288-297.  
[PUBMED](#) | [CROSSREF](#)
43. Kim JH, Sun W, Han DW, Moon HJ, Lee J. iNSC suppress macrophage-induced inflammation by repressing COX-2. *In Vitro Cell Dev Biol Anim*. 2015;51(2):157-164.  
[PUBMED](#) | [CROSSREF](#)
44. Kim JH, Lee J. Induced neural stem cells protect neuronal cells against apoptosis. *Med Sci Monit*. 2014;20:2759-2766.  
[PUBMED](#) | [CROSSREF](#)
45. Tfilin M, Sudai E, Merenlender A, Gispán I, Yadid G, Turgeman G. Mesenchymal stem cells increase hippocampal neurogenesis and counteract depressive-like behavior. *Mol Psychiatry*. 2010;15(12):1164-1175.  
[PUBMED](#) | [CROSSREF](#)
46. Wolff M, Vann SD. The cognitive thalamus as a gateway to mental representations. *J Neurosci*. 2019;39(1):3-14.  
[PUBMED](#) | [CROSSREF](#)
47. Bezudnaya T, Keller A. Laterodorsal nucleus of the thalamus: a processor of somatosensory inputs. *J Comp Neurol*. 2008;507(6):1979-1989.  
[PUBMED](#) | [CROSSREF](#)